Protein-Induced Membrane Disorder: A Molecular Dynamics Study of Melittin in a Dipalmitoylphosphatidylcholine Bilayer

Michal Bachar and Oren M. Becker
School of Chemistry, Tel Aviv University, Ramat Aviv, Tel Aviv 69978, Israel

ABSTRACT A molecular dynamics simulation of melittin in a hydrated dipalmitoylphosphatidylcholine (DPPC) bilayer was performed. The 19,000-atom system included a 72-DPPC phospholipid bilayer, a 26-amino acid peptide, and more than 3000 water molecules. The N-terminus of the peptide was protonated and embedded in the membrane in a transbilayer orientation perpendicular to the surface. The simulation results show that the peptide affects the lower (intracellular) layer of the bilayer more strongly than the upper (extracellular) layer. The simulation results can be interpreted as indicating an increased level of disorder and structural deformation for lower-layer phospholipids in the immediate vicinity of the peptide. This conclusion is supported by the calculated deuterium order parameters, the observed deformation at the intracellular interface, and an increase in fractional free volume. The upper layer was less affected by the embedded peptide, except for an acquired tilt relative to the bilayer normal. The effect of melittin on the surrounding membrane is localized to its immediate vicinity, and its asymmetry with respect to the two layers may result from the fact that it is not fully transmembranal. Melittin's hydrophilic C-terminus anchors it at the extracellular interface, leaving the N-terminus "loose" in the lower layer of the membrane. In general, the simulation supports a role for local deformation and water penetration in melittin-induced lysis. As for the peptide, like other membrane-embedded polypeptides, melittin adopts a significant 25° tilt relative to the membrane normal. This tilt is correlated with a comparable tilt of the lipids in the upper membrane layer. The peptide itself retains an overall helical structure throughout the simulation (with the exception of the three N-terminal residues), adopting a 30° intrahelical bend angle.

INTRODUCTION

Biological membranes consist of a lipid matrix (the lipid bilayer) in which molecules, such as proteins and cholesterol, are embedded. When a protein is incorporated into the lipid bilayer it may influence the membrane phase behavior, affecting the membrane dynamics and modifying its biological function. Thus the manner in which the presence of proteins in phospholipid bilayers affects the properties of the membrane has for a long time been the focus of intensive research. Of particular interest is the difference between "boundary" phospholipids, i.e., lipids in direct contact with the embedded protein, and the more distant "bulk" lipids.

Lipid bilayers composed of a single lipid species undergo several different types of phase transitions (Geve and March, 1987; Mouritsen, 1991; Mouritsen and Biltonen, 1993). The transition that is believed to have a substantial effect on membrane function is the main gel-to-fluid phase transition. This phase transition takes the membrane from a lower-temperature gel phase, characterized by acyl-chain order, to a higher-temperature fluid phase characterized by conformational disorder and fast lateral diffusion. This phase behavior is further complicated when the bilayer is composed of more than a single lipid species and when integral membrane proteins are present. It is sensitive to molecular interactions in the lipid bilayer system, to temporal fluctuations of the lipids (as seen, for example, by fluorescence experiments; Ruggiero and Hudson, 1989), as well as to the presence of heteromolecules.

The overall effect of incorporating integral proteins into membranes is a significant change in the phase equilibria (Mouritsen and Biltonen, 1993), involving structural changes in the adjacent lipid molecules. Common experimental probes to this effect are spectroscopic order parameters, which refer to the conformational order of the acyl chains. Early electron spin resonance studies indicated that on the experiment's time scale, lipids around a protein are ordered in a way that is different from the way in which bulk lipids are ordered (Jost et al., 1973). This difference between the two types of lipids disappears on the much longer time scale of NMR experiments (Deveaux and Siegneuret, 1985).

Theoretical investigations of lipid-protein interactions were limited for a long time to simplified models. Monte Carlo simulations of model systems, composed of a schematic "cylindrical" protein in a simplified carbohydrate monolayer, have shown very little effect of the "protein" on the order parameter of the neighboring lipids (Scott, 1986). Similar simulations of cholesterol in the model monolayers (Scott and Kalaskar, 1989) had indicated that the cholesterol affects the upper portion of the chains, constraining their conformational freedom, while making the lower termini of C-16 and C-18 chains a little less ordered than bulk chains. The reduced order at the chain termini was not observed with shorter C-14 chains. In a different study the insertion of

Received for publication 1 October 1998 and in final form 30 November 1999.

Address reprint requests to Dr. Oren M. Becker, School of Chemistry, Tel Aviv University, Ramat Aviv, Tel Aviv 69978, Israel. Tel.: 972-3-640-7599; Fax: 972-3-640-9293; E-mail: becker@sapphire.tau.ac.il.

0006-3495/00/03/1359/17 $2.00

peptides into membranes was studied using Monte Carlo and a simplified model (Milik and Skolnick, 1993). With the increase in computer power, model membrane simulations were gradually replaced by detailed all-atom molecular dynamics (MD) studies of phospholipid bilayers. MD simulations of bilayer systems began with modest model systems (van der Ploeg and Berendsen, 1982) and improved with time, reaching various solvated bilayers of more than 100 phospholipids (Alper and Stouch, 1995; Berger et al., 1997; Chiu et al., 1995; Damodaran and Merz, 1994; Feller et al., 1997; Heller et al., 1993; Lopez Cascales et al., 1996; Marrink et al., 1996, 1998; Pastor, 1994; Tieleman and Berendsen, 1996; Tieleman et al., 1997). These simulations reproduce experimental results as well as probe at an atomic level the interactions between the bilayer and the surrounding water molecules.

Recently the first detailed all-atom MD simulations of peptides in a phospholipid bilayer were reported. Damodaran et al. (1995) reported a simulation of a small tripeptide in a 16 × 2 dipalmitoylphosphatidylcholine (DMPC) bilayer. Roux, Woolf, and collaborators have performed a series of studies on several transmembrane helices embedded in a solvated DMPC bilayer. In these simulations the peptides, gramicidin A (Woolf and Roux, 1996), a model amphiphilic helix (Belohorcova et al., 1997), and individual helices from bacteriorhodopsin (Woolf, 1997; Woolf, 1998), were surrounded by 8 × 2 or 12 × 2 DMPC phospholipids in a hexagonal boundary and capped by water molecules. In separate studies Shen et al. (1997) simulated a single transmembranal polyalanine helix in a solvated 16 × 2 DMPC bilayer, and Tieleman et al. (1999) studied the alamethicin channel-forming peptide in a palmitoyloleoylphosphatidylcholine bilayer. The primary focus of these studies was the effect of the membrane on the properties of the embedded polypeptide. It is only in recent years, with the increase in computer power, that the complementary question, i.e., the effect of the protein on the embedding membrane, is being addressed. Very recently an unprecedented large system, consisting of the large OmpF porin trimer and a hydrated bilayer consisting of 318 palmitoyloleoylphosphatidylethanolamine (POPE) phospholipids was simulated by Tieleman and Berendsen (1998). An in-depth analysis of the protein's effect on the embedding phospholipids was recently reported by Tieleman et. al (1998), who studied the proteins OmpF, influenza M2, and alamethicin in a large POPE membrane.

The focus of the present study is the reciprocal effect of a membrane-embedded peptide, exemplified by the peptide melittin, on the properties of the host membrane and vice versa. The 26-amino acid peptide melittin is the principal toxic component of the venom of the honey bee (Terwilliger and Eisenberg, 1982). It spontaneously binds to lipid bilayers and acts as a lytic agent (Vogel and Jähnig, 1986). Three mechanisms for the lytic activity of melittin have been proposed (Dempsey, 1990): 1) lysis is due to melittin-induced formation of ion-permeable water pores (Tosteson et al., 1985); 2) lysis results from the perturbation of the lipid bilayer due to the presence of the peptide in the headgroup region (DeGrado et al., 1982); 3) lysis occurs as a result of melittin aggregation (Dufourc et al., 1986). It seems that the first two mechanisms are best supported by the experimental data, although to a lesser extent the third mechanism also has experimental support. In fact, the first two mechanisms are probably intimately connected, as water penetration can be helped by structural perturbations at the bilayer's surface. For example, MD simulations (Marrink and Berendsen, 1994) have shown that the rate of water translocation through the bilayer is limited by the interfacial region near the glycerol. Water penetration can increase by the formation of defects at the interface, possibly by a membrane-embedded peptide.

In any case, regardless of the lysis mechanism assumed, the molecular details of these mechanisms are still unclear. In particular, it is unclear how lysis is related to the change in melittin's membrane-binding orientation. Several researchers have suggested that partial translocation of melittin, from the initial binding orientation parallel to the membrane surface to a transbilayer orientation in the hydrophobic core, is involved in lysis (Berneche et al., 1998; Bradshaw et al., 1994; Weaver et al., 1992). Based on neutron scattering measurements at different bulk pH, Bradshaw et al. (1994) proposed that melittin with an unprotonated N-terminus binds parallel to the membrane surface, whereas melittin with a protonated N-terminus binds in a transbilayer way. Interconversion between the two binding modes appears to be possible under equilibrium conditions.

A characterization at the molecular level of the association of melittin with membranes and its influence on the surrounding lipid phase is necessary for a better understanding of the microscopic mechanism involved in the lytic event. Very recently, an MD simulation of melittin in a bilayer environment was reported by Berneche et al. (1998). In that simulation melittin with an unprotonated N-terminus was bound parallel to a DMPC membrane surface (although during the simulation the N-terminus penetrated into the upper layer of the membrane). Upon protonation of the N-terminus it was found that water penetration into the bilayer increases significantly.

Unfortunately, interconversion between parallel and perpendicular melittin orientations is not possible on the time scale of MD simulations (even though the simulated membrane is in its Lα phase). Thus in the present study we have simulated the complementary scenario, in which melittin is already embedded in the membrane adopting its transbilayer orientation. In accord with neutron-scattering measurements (Bradshaw et al., 1994), the N terminus of the peptide in the present simulation was protonated. In all, the simulated system consists of the peptide melittin embedded in a 36 × 2 DPPC bilayer at its Lα phase (72 1,2-dipalmitoyl-3-*sn*-phosphatidylcholine phospholipids), capped by a 40-Å wa-

ter layer (more than 3000 water molecules), under periodic boundary conditions. In principle, this system is large enough to study the effect of the peptide on the properties of non-nearest-neighbor phospholipids.

It is important to note that even at this so-called transbilayer orientation melittin does not span the bilayer from side to side. In fact, it spans no more than two-thirds of the bilayer's width. This means that melittin is anchored to only one of the two membrane's surfaces (the extracellular side), leaving the N-terminus free in the membrane's hydrophobic core. In this respect, the melittin/membrane system is significantly different from other peptide/membrane systems studied by MD, in which the peptides fully span the membrane from one side to the other and are anchored on both sides on the bilayer (Belohorcova et al., 1997; Shen et al., 1997; Tieleman et al., 1999; Woolf, 1997, 1998; Woolf and Roux, 1996).

THE SIMULATION

Melittin

Melittin is a 26-amino acid protein (Gly-Ile-Gly-Ala-Val^{5}-Leu-Lys-Val-Leu-Thr^{10}-Thr-Gly-Leu-Pro-Ala^{15}-Leu-Ile-Ser-Trp-Ile^{20}-Lys-Arg-Lys-Arg-Gln^{25}-Gln) and is the principal toxic component of the venom of the honey bee (Dempsey, 1990; Terwilliger and Eisenberg, 1982); it has a cationic character. The 20 amino acids at the N-terminus part of melittin have a predominantly hydrophobic character, whereas the six amino acids at the C-terminus are very hydrophilic and basic. Melittin is soluble in both water and methanol. In water it is either monomeric or tetrameric and is shaped like a bent rod, in which the bend in the molecule is induced by residue Pro^{14} (Pastore et al., 1989; Vogel and Jähnig, 1986). In methanol melittin is monomeric and helical, with a bend angle of $\sim 20^{o}$, significantly smaller than the 60^{o} angle observed in water (Bazzo et al., 1988). Various experimental studies have shown that melittin is helical in a lipid environment. The orientation of melittin in a phospholipid bilayer appears to be complex and is sensitive to experimental conditions (Milik and Skolnick, 1993). When the peptide is membrane bound, residue Trp^{19} is located approximately at the height of the C1 atoms of the lipid hydrocarbon chains (Vogel and Jähnig, 1986), leaving the six C-terminus amino acids outside of the hydrophobic region, allowing them to interact with the polar headgroups and the surrounding water. As described above, the orientation of membrane-bound melittin is uncertain (Dempsey, 1990). Several experimental results indicate that the peptide is oriented roughly perpendicular to the membrane surface (Vogel, 1987; Vogel and Jähnig, 1986), although there are also results (in the fluid phase of the bilayer) that indicate a parallel orientation (Dempsey, 1990). Recent neutron scattering measurements with melittin at different bulk pH (Bradshaw et al., 1994) suggest that melittin with unprotonated N-terminus binds parallel to the membrane surface, whereas melittin with a protonated N-terminus binds in a transbilayer way. Support for the role of the perpendicular orientation in membrane lysis is given by the requirement for a specific cationic C-terminal that anchors the molecule in the vertical orientation (Habermann and Kowallek, 1970; Manjunatha-Kini and Evans, 1989), as well as by the fact that shortened N-terminal sequences are very poor lytic agents (Gevod and Birdi, 1984). The ambiguity regarding peptide orientation pertains also to computational studies that used simplified models to represent the melittin-membrane system. In one study the preferred orientation of the helix was found to be roughly perpendicular to the bilayer surface (Milik and Skolnick, 1993), whereas another study indicated that melittin can access a wide range of orientations, from perpendicular to almost parallel (Ducarme et al., 1998).

The initial melittin coordinates were taken from the x-ray structure of Terwilliger and Eisenberg (protein data bank entry 2mlt; Terwilliger and Eisenberg, 1982). To prepare the molecular model for interfacial positioning at the membrane interface, the six C-terminal amino acids were minimized separately, using a water dielectric constant (the rest of the peptide was fixed), and the 20 N-terminal amino acids were minimized separately, using a hydrophobic dielectric constant. The CHARMM molecular mechanics program (Brooks et al., 1983) and force field were used (MacKerell et al., 1998).

Pure phospholipid bilayer

In general, melittin's lysis activity strongly depends on membrane composition. Membranes with longer hydrocarbon chains are less affected by the lysis activity of melittin (Bradrick et al., 1995), while bilayers of zwitterionic lipids are more affected compared to bilayers of charged phospholipids (Monette and Lafleur, 1995). These two considerations led us to simulate melittin in a 1,2-dipalmitoyl-3-*sn*-phosphatidylcholine (DPPC) bilayer. DPPC is a zwitterionic phospholipid with a medium tail consisting of 16 carbons. It is of a length appropriate to the study of the effect of melittin and yet is still relevant to realistic biological membranes, which typically include 16–20- or 22-carbon-long phospholipids. In addition, DPPC is one of the best studied phospholipids, by both experiment and simulation, and has been termed the "benchmark" of lipid simulations (Tieleman et al., 1997). Thus the well-characterized DPPC system sets a clear baseline for studying the effect of the embedded peptide on membrane properties.

The DPPC phospholipid bilayer model used in this study is based on the model developed by Feller and Pastor (Feller et al., 1997). Molecular dynamics simulations of this system under NPAT conditions, constant normal pressure, and fixed surface area (Feller and Pastor, 1996; Feller et al., 1997), involving periodic boundary conditions, were shown

to be reliable. These simulations agree with experimental results, such as deuterium order parameter and electron density profiles. Feller and Pastor's results also support the validity of the empirical phospholipid force field included in the CHARMM 22b4 parameter set (MacKerell et al., 1998; Schlenkrich et al., 1996). The pure membrane model includes 72 DPPC phospholipid molecules arranged in a square 36 × 2 bilayer (with periodic boundary conditions) corresponding to the biologically active L_α phase of the membrane. The bilayer size is 47.6 Å × 47.6 Å × 68 Å, set to allow the area per phospholipid headgroup to be 62.9 $Å^2$. This value for the area per headgroup was suggested by Nagle et al. (1996) and was shown by Feller and Pastor to best reproduce experimental results (Feller et al., 1997). The bilayer is flanked by a 30-Å layer of TIP3P water (using periodic boundary conditions in the direction normal to the bilayer). A total of 2509 water molecules were included in the pure membrane simulation. The initial conformation of the equilibrated bilayer was from Feller and Pastor (Feller et al., 1997). An additional 100 ps of dynamics was performed on the pure membrane model, to obtain a baseline to which the melittin/bilayer system will be compared.

The CHARMM molecular dynamics program (Brooks et al., 1983) and the CHARMM all-atom phospholipid force field (Schlenkrich et al., 1996) were used. The SHAKE algorithm was applied to all bonds involving hydrogen atoms, and a 2-fs time step was used. The nonbonded Lennard-Jones interactions were switched to zero over the region 12–14 Å. Ewald summation was used for the calculation of electrostatics (Feller et al., 1996). The real space summation was truncated at 12 Å, using $\kappa = 0.210$ $Å^{-1}$. The reciprocal space summation was truncated at $k_{xx} = k_{yy} = 6$ and $k_{zz} = 9$. Three-dimensional periodic boundary conditions were applied, and the cell length normal to the membrane was allowed to adjust to maintain a constant normal pressure of 1 atm, using a Langevin piston algorithm (Feller et al., 1995). A mass of 500 amu and a collision frequency of 5 ps^{-1} were used for the pressure piston.

The simulation temperature of 320 K, which was controlled by a Nose-Hoover thermostat, is above the gel-liquid phase transition temperature for DPPC (314.5 K in multilamellar vesicles) (Koynova and Caffrey, 1998). This temperature ensures that the system is at the biologically relevant, fully hydrated liquid crystalline Lα phase of the bilayer, yet is still low enough to ensure the stability of the embedded peptide.

Combined melittin/bilayer system

Before we introduced the peptide into the membrane, the water layer had to be broadened to ensure full solvation of the peptide's C-terminus and to prevent an artificial interaction of the peptide with the lower membrane surface (through the periodic boundary conditions). For this end a 12-Å slab of water from the center of the water layer was copied and reintroduced next to the original slab, allowing a small overlap between the new layer and the original layer. The combined water layer was then minimized for 200 steepest descent steps, which was sufficient to relax most of the van der Waals overlaps. The excess water spreads uniformly during the equilibration process, resulting in a water layer of ~40 Å, with a uniform water density similar to that of the original system. Attempts to extend the water layer without an overlap region resulted in density fluctuations and cavity formation. At the end of this process the system included 3207 water molecules, and the dimensions of the extended system were 47.6 Å × 47.6 Å × 80 Å.

An important issue in modeling a combined peptide/membrane system is the initial placement and orientation of the embedded peptide. In this study, melittin was introduced into the membrane in a vertical orientation, i.e., perpendicular to the membrane surface. This initial placement means that the simulation will not address the process of peptide insertion or the change in orientation from parallel to transbilayer (these processes are too slow and cannot be studied on the time scale of MD simulations). Rather we study the reciprocal effects between peptide and membrane after the peptide has already been embedded in the membrane in the transbilayer orientation. Following the neutron-scattering measurements of Bradshaw et al. (1994), which proposed that melittin with an unprotonated N-terminus binds parallel to the membrane surface, whereas melittin with an protonated N-terminus binds in a transbilayer way, the N-terminus of melittin in the present study was protonated. Practically, the melittin peptide was placed in the cavity formed by removing two DPPC phospholipids from the center of the upper layer. It was then rotated around its z axis to find the optimal rotational orientation that would best fit the cavity. The orientation with the least amount of bad contact, i.e., with the lowest van der Waals repulsion, was selected as the starting conformation. The vertical positioning was based on the experimental observation (Vogel and Jähnig, 1986) that the peptide is practically perpendicular to the bilayer plane with residue Trp^{19} slightly above the plane defined by the C1 carbons of the lipid hydrocarbon chains. Thirty-six water molecules were removed from the model because of overlaps with the peptide C-terminus amino acids. Two hundred steepest descent minimization steps of the peptide alone, followed by 2000 steepest descent steps of the combined model (peptide + phospholipids + water), were required to relax the system and remove practically all bad contacts. At the end of this process the peptide was positioned nicely in the membrane. No significant cavities were formed because of the insertion process (as indicated by the fractional free volume discussed below). Although the embedded peptide also interacts with the lower layer of phospholipids, no special treatment was assigned to it because the peptide penetration is limited to the low-density region, near the membrane midplane, of this layer (see the density profiles below). The method used in this study for placing

the peptide in the membrane resembles the method of Shen et al. (1997), which was later adopted by Tieleman and Berendsen (Tieleman and Berendsen, 1998; Tieleman et al., 1999). In both methods the peptide is inserted into a precreated cavity in the membrane (although in the present study there was no need for an additional cylindrical repulsive force to expand the cavity). In the studies of Roux, Woolf ,and collaborators, phospholipids were added around a preexisting helix (Belohorcova et al., 1997; Woolf, 1997, 1998; Woolf and Roux, 1996).

The complete combined model included the melittin peptide, 70 phospholipids, and 3171 water molecules, a total of 19,049 atoms all together. After the initial preparation of the model it was gradually heated from 100 K to 320 K over a 15-ps period. The combined peptide-membrane-water system was reequilibrated for 200 ps (recall that the pure membrane was already equilibrated), followed by a 300-ps production run at 320 K, totaling 500 ps of simulation. Conformation snapshots of the trajectory were saved every 0.5 ps throughout the simulation. All simulations were performed on an IBM SP2 super computer, at a rate of 70 min/ps, using 16 processors in parallel.

The length of the simulation was dictated by available computer power and the assumed time scale of the processes of interest. Previous simulations of membrane systems indicated that relaxation of perturbed bilayers takes place on the 200-ps time scale (Feller et al., 1997), so we expect the membrane to adjust to the presence of the peptide well within the time scale of the simulation. Clearly, the simulation length is not sufficient for the study of a possible orientational reorganization of the helix from the perpendicular to the parallel orientations. Significantly longer lime scales are required for such a study.

Fig. 1 shows a detailed view of the combined system after 500 ps of molecular dynamics (about half of the membrane phospholipids "in front" of the peptide were removed to obtain a clearer view).

RESULTS

Density profile of the combined system

Molecular density profiles present distributions of certain molecular components, atom or chemical groups, along the axis perpendicular to the membrane surface. Previous studies (Tieleman et al., 1997) showed that density profiles calculated for pure membrane bilayers are characterized by three phenomena: 1) a rough membrane surface characterized by a broad headgroup region, ~10–13 Å wide; 2) water penetration that reaches deep into the headgroup region and up to the carbonyl groups of the membrane; 3) a wide distribution of the CH_3 segments, indicating that tails can fold back on themselves to give considerable CH_3 density even far from the membrane midplane.

The density profiles in Fig. 2 are calculated for the combined membrane-peptide-water system. Unlike standard density profiles, which show the density at the level of the atoms (atoms/A^3), the density plots of Fig. 2 are normalized and are calculated at the level of chemical groups. This means that the area under each density profile is normalized to one. These normalized density plots were chosen because they highlight the membrane interface (the phosphate group) and the membrane midsection (CH_3 groups). Fig. 2 shows normalized density plots for key chemical groups in the bilayer system (phosphate, CH_2, CH_3, and water) averaged over the last 300 ps of the dynamics simulation. The atomic density of the embedded peptide is also shown. It should be noted that the values in the normalized density plots are quite different from those in standard density plots. For example, in this system the normalized density of bulk water is 0.023. Translated back to standard density, this normalized value is equal to the expected experimental density of bulk water (0.033 molecule/A^3).

Fig. 2 indicates that the density of the different membrane components in the combined system is similar to that of the pure membrane. In particular, the width of the interface, as reflected by the width of the density peak of the phosphorous atoms, is 12 Å, similar to the values calculated for pure bilayers (10–13 Å) (Tieleman et al., 1997). A slightly broader estimate of the surface corrugation is obtained from the width of the peaks that correspond to the glycerol carbon atoms (not shown in Fig. 2), which in the combined system is ~14 Å. Finally, the very broad CH_3 peak characteristic of pure bilayers is also observed in the combined system (~14 Å on both sides of the membrane midplane). Determining the average width of the membrane depends on the chemical group used to define the membrane surface. A definition based on the peak density of the glycerol carbon atoms (not shown in Fig. 2) yields an average membrane width of 33 ± 2 Å, whereas a definition based on the phosphate groups yields an average membrane width of 38 ± 2 Å (the standard deviation of each phosphate peak ±1 Å).

The peptide density profile is, of course, a unique feature of the combined system. Fig. 2 shows that the hydrophilic C-terminus of the peptide extends ~12 Å above the average membrane surface (defined by the phosphorous atoms). The hydrophobic N-terminus of the peptide, on the other hand, penetrates ~9 Å into the lower half of the bilayer. The large number of water molecules flanking the membrane is clearly seen.

Peptide structure

The reciprocal effect of the membrane on the peptide and of the peptide on the membrane are the focus of the present study. Although these effects are coupled, we shall first discuss the effects of the membrane on the structure of the peptide, following which the peptide's effect on the struc-

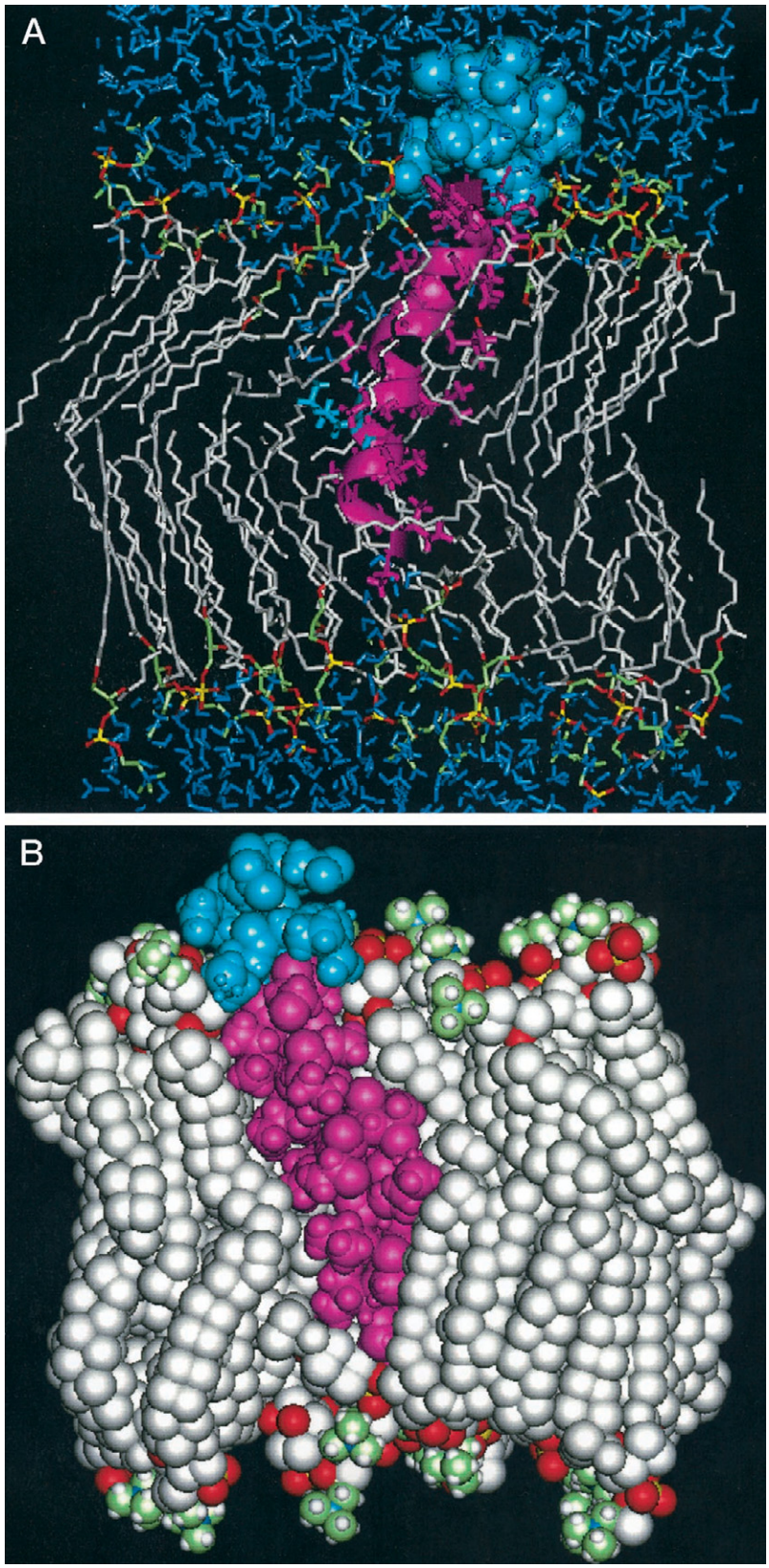

FIGURE 1 (*A*) A detailed view of the combined melittin/membrane/water system after 500 ps of molecular dynamics. The hydrophilic C-terminus of the peptide is colored blue (using a space-filling representation), and its hydrophobic part is colored purple (showing its helical structure). To obtain a clearer view, about half of the membrane phospholipids "in front" of the peptide as well as the hydrogen atoms of the acyl chains are not shown. The overall tilt of the peptide and the upper layer lipids is clearly seen. (*B*) A spaced-filling model of the peptide in the membrane (about half of the bilayer's phospholipids as well as the water molecules are not shown).

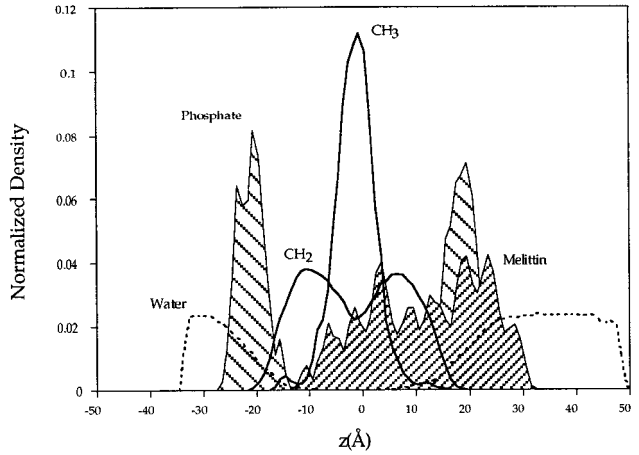

FIGURE 2 Normalized density profiles of all key chemical groups in the combined membrane-peptide-water system (P atoms, CH_2, CH_3, water, and the peptide) averaged over the last 300 ps of the dynamics simulation. These density profiles are similar to those calculated for a pure membrane. Note the broad membrane interface (12 Å, as reflected by the density of the phosphorous atom) and a very broad CH3 peak (~14 Å on both sides of the membrane midplane). Densities are calculated as chemical groups per unit volume, except for the melittin, for which density is calculated as atoms per unit volume.

tural properties of the membrane will be presented. The structural properties of the embedded peptide are gauged through the following properties: the structural integrity of the peptide, its intrahelix bend angle, the tilt of the peptide relative to the membrane normal, and its vertical position relative to the membrane surface.

Structural integrity of the peptide

The issue of melittin's "structural integrity" corresponds to the question of whether its overall helical structure remains intact in the phospholipid bilayer. In the present work the helical structure is characterized simply by the peptide's backbone (ϕ,ψ) dihedral angles, which in an ordered α-helix are in the vicinity of -60^o. Fig. 3 shows the values obtained for each of the peptide's backbone dihedral angles during the 500 ps of the simulation (sampled every picosecond). As can be seen, the majority of both ϕ (Fig. 3 *A*) and ψ (Fig. 3 *B*) dihedral angles reflect a very stable α-helical structure, with values in a 30^o range around -65^o for the ϕ dihedral angles and values in a 30^o range around -45^o for the ψ dihedral angle. The standard deviation of individual dihedral angles was between $\pm 7^o$ and $\pm 12^o$. The main exception to the structural stability of the peptide is the three N-terminal residues (Gly^1-Ile^2-Gly^3), whose backbone dihedral angles deviate from helical with higher than standard fluctuations (in particular, Gly^3, with values of $-17.2^o \pm 40^o$ and $-71.0^o \pm 29^o$ for the ϕ and ψ dihedral angles, respectively). This "unwinding" of the flexible helix terminus is strongest in residues Gly^1 to Gly^3, but can also be seen to affect the ψ dihedral angle of residues Ala^4 ($-29.6^o \pm 12^o$) and Val^5 ($-18.8^o \pm 17^o$). It is also manifested in a increased level of fluctuations in the ϕ dihedral angle of residue Ala^4 ($\pm 13^o$). On the time scale of the simulation, this structural perturbation does not propagate further along the helix. The flexibility and "unwinding" of the N-terminus may be explained in two ways. The first is that the "unwinding" is due to its location in the relatively low density and structureless interior of the membrane, especially given the presence of two Gly residues in this section of the peptide. A second explanation may be that the "unwinding" is caused by the presence of penetrating water molecules (Bachar and Becker, 1999). A similar loss of the α-helical character of the N-terminus segment Gly^1 to Val^5 was observed in the study of Berneche et al. (1998) after protonation of the N-terminus and penetration of water into the bilayer (peptide orientation parallel to the membrane-solvent interface). Further support for the water-induced "un-

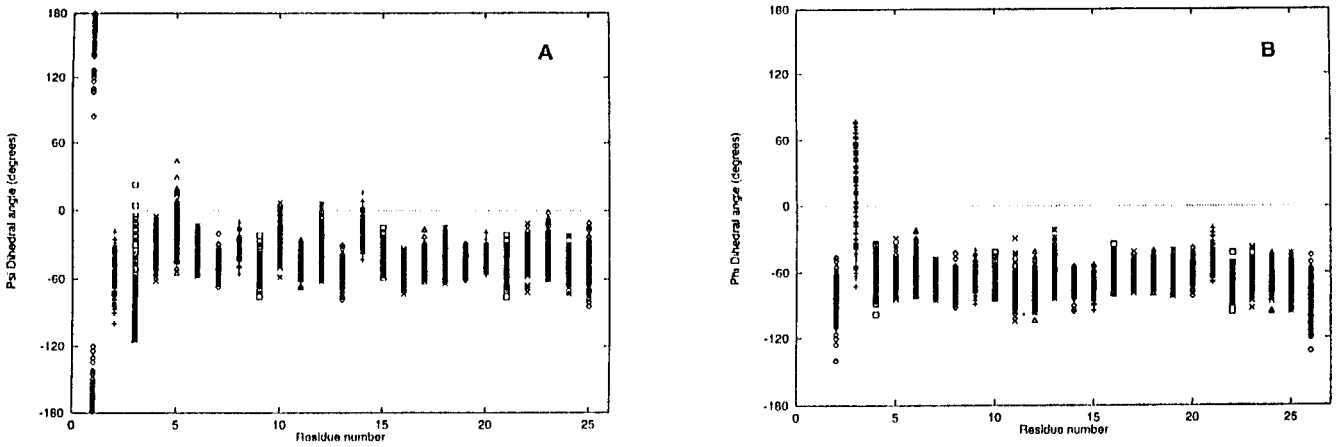

FIGURE 3 The backbone ϕ (*A*) and ψ (*B*) dihedral angles of all 26 melittin residues. Each dihedral angle is sampled 500 times (every picosecond). In an ordered α-helix both dihedral angles are close to -60^o. Except for the peptide's N-terminus, the α-helical structure of the peptide remains intact throughout the simulation.

winding" can be obtained from a previous computational study based on a simplified model (Milik and Skolnick, 1993), which found that the helix is better defined at the membrane-embedded N-terminus of melittin than the surface-anchored C-terminus.

No special flexibility is observed at the intrahelix bend region (residues Thr^{11}-Pro^{14}), except possibly for a little more flexibility in the ψ dihedral angle of residues Thr^{10} and Gly^{12} ($\pm 12.2^{o}$ and $\pm 13.7^{o}$, respectively) and, as expected, a different value for Pro^{14} ($\psi = -17.3^{o} \pm 10.7^{o}$). The stability of the bend region agrees with the observation that the intrahelical bend angle fluctuates very little, on the order of $\pm 4^{o}$, around its average value (see below). Fig. 3 also shows that the helical structure at the peptide's C-terminus is kept intact throughout the simulation. This stability is due to the many specific interactions that it forms with the phospholipid headgroups.

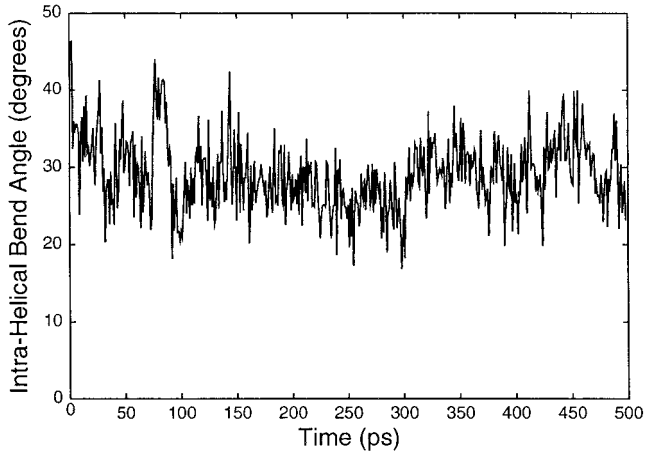

FIGURE 4 The bend angle between the two sections of the melittin helix as a function of time, during the 500 ps of the dynamics simulation.

Intrahelical bend

The membrane-embedded helix of melittin comprises two "rods" connected by a characteristic kink between residues Thr^{10} and Pro^{14}. The intrahelical bend angle of melittin was determined to be 20^{o} in methanol (Bazzo et al., 1988) but 60^{o} in water (Terwilliger and Eisenberg, 1982). Molecular dynamics simulations of melittin in vacuum also resulted in an intrahelical bend angle of $\sim 20^{o}$ (with large fluctuations) (Pastore et al., 1989).

In the present study the intrahelical bend angle is defined as the angle between two axes, one characterizing the lower "rod" of the helix (axis defined between the center of mass of the backbone atoms of residues 5–8 and the center of mass of the backbone atoms of residues 7–10) and another axis characterizing the upper "rod" (a similarly defined axis between the backbone center of mass of residues 14–17 and 17–20). Because the simulation started from the x-ray structure 2mlt (Terwilliger and Eisenberg, 1982), the initial intrahelical bend angle was 60^{o}, as in water. However, within less than 10 ps of dynamics the intrahelical bend angle changed to $\sim 30^{o}$ and remained at that value throughout the dynamic simulation. Fig. 4 shows the intrahelical bend angle of melittin during the 500 ps of the dynamics simulation. The average value of this bend angle, during the last 300 ps of the simulation, is $29.4^{o} \pm 4.1^{o}$. As expected, this bend angle is closer to the value in methanol than to that in water. A similar bend angle of $35^{o} \pm 5^{o}$ was reported by Berneche et al. (1998) for melittin with an unprotonated N-terminus bound parallel to the surface.

Helix tilt relative to membrane normal

An important property that characterizes membrane-embedded helices is their orientation relative to the membrane plane. In the case of melittin, both experimentally and theoretically, the peptide's orientation relative to the bilayer normal is not clear. As reviewed above, some experiments indicated a perpendicular orientation, while others indicated a parallel orientation. The results obtained from simplified computational models were also inconclusive, with one study pointing toward a perpendicular orientation and another indicating a broad range of possible orientations. This complex scenario probably indicates that melittin adsorbs to the membrane surface (parallel orientation) before its insertion into the membrane (perpendicular orientation).

In the present study, the initial orientation of the peptide was set perpendicular to the membrane surface, to mimic the postinsertion conformation. During the course of the dynamics the peptide's orientation changed and it acquired a tilt relative to the membrane normal. This tilt is clearly visible in Fig. 1, which shows the final conformation of the system after 500 ps of dynamics. Fig. 5 depicts the tilt angle between the upper part of the membrane-embedded helix of

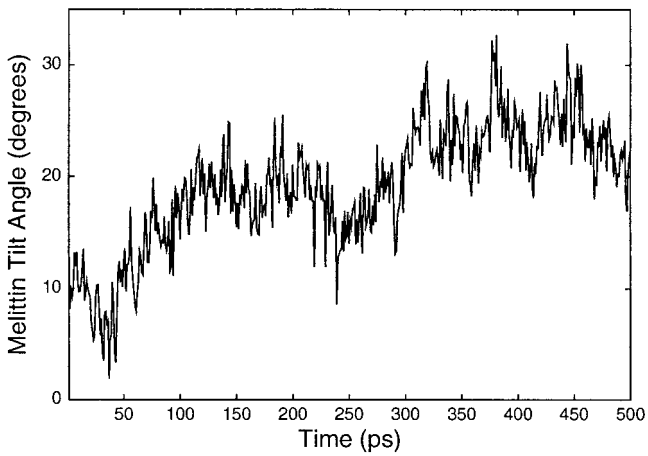

FIGURE 5 The orientation of melittin in the membrane as a function of time. The tilt angle is calculated between the upper part of the melittin helix (residues 14–21) and the normal to the membrane surface (z axis).

melittin (defined as residues 14–21) and the normal to the membrane surface (z axis). The first change in orientation occurred very quickly during the initial heating of the system, when the peptide attained a small 10° tilt angle. After the initial change, the peptide's tilt fluctuates strongly and gradually increases over the rest of the simulation. The average tilt angle over the last 300 ps of the simulation is $21.8^{o} \pm 4.2^{o}$ relative to the membrane normal. A slightly higher value of $23.9^{o} \pm 3.0^{o}$ is obtained from averaging only over the last 200 ps of the simulation.

The tilting of melittin in the membrane is similar to the tilt observed for transmembrane helices. Simulations of two different transmembrane helices in a DMPC bilayer (Belohorcova et al., 1997; Shen et al., 1997) showed that the orientation of these helices, relative to the membrane normal, fluctuates significantly, and they obtain a tilt angle of up to 30°. Clearly, much longer simulations are needed before this short time scale tilt can be compared to experimental results, which average the tilting process on much longer time scales.

Vertical position

An interesting question that may reflect on the quality of the simulation is whether the vertical position of the peptide has changed during the simulation. A large variation in this quantity could indicate that the initial vertical positioning of the peptide, with residue Trp^{19} near the plane defined by the phospholipid C1 atoms, was inappropriate. During the 500 ps of the simulation there was practically no change in the vertical position of the peptide relative to the average surface of the membrane nor any perceived change in the overall width on the membrane (although deformation of the surface at the intracellular side makes it hard to determine the exact width near the peptide; see below). Calculations of the average z coordinate of the topmost residue Gln^{26} showed no vertical drift and only relatively small fluctuations of ± 0.7 Å around its average position. Even smaller fluctuations of ± 0.5 Å were observed for residue Trp^{19}, which also did not change its vertical position during the simulation. These results indicate that the vertical position of the peptide at the membrane interface is stable on the time scale of the simulation. No conclusions regarding the stability of this vertical position over longer time scales can be drawn.

Membrane Structure

Membrane order parameter

Deuterium order parameters, obtained from NMR experiments, are often used to probe the structure of lipid bilayer membranes. The order parameter, S_{CD}, is given by

$$S_{CD} = \langle 3/2 \cos^2\theta - 1/2 \rangle \quad (1)$$

where θ is the angle between the CD bond vector and the bilayer normal, and the brackets denote an average over time over all of the lipids (or over a subset of the membrane lipids). The value of S_{CD} quantifies the degree of reorientation that occurs on the NMR time scale, i.e., how ordered the molecules are and their average orientation with respect to their bilayer normal. A vector undergoing isotropic rotation will have an order parameter of zero. Typical values of S_{CD} for fluid-phase lipid bilayers range from ~ -0.2 near the headgroups to near zero in the terminal methyl groups. Order parameters along the hydrocarbon chains of a fully hydrated DPPC bilayer were determined experimentally at 50°C (Douliez et al., 1995; Seelig and Seelig, 1974). A useful comparison parameter is the average of the CH order parameters in the plateau region between C4 and C8, $\langle S_{CD} \rangle_{[4,8]}$. For DPPC the experimentally determined value of this parameter is in the range of 0.209–0.217. This value was reproduced in the MD simulations of Feller et al. (1997) at 50°C ($\langle S_{CD} \rangle_{[4,8]} = 0.215$), as well as in our simulation of a pure DPPC system ($\langle S_{CD} \rangle_{[4,8]} = 0.209 \pm 0.006$). Individual fluctuations in the order parameter of individual carbon atoms are on the order of 0.1.

Because melittin does not span the membrane from side to side, its effect on the order parameter of phospholipid in the upper (i.e., extracellular) layer has to be studied separately from its effect on the lower (i.e., intracellular) layer. Furthermore, to study the effect of peptide proximity on the order parameter of the phospholipids, these were grouped into three equal size "tiers" based on their distance from the peptide. The first group includes the 11 phospholipids closest to the peptide (the distance in the horizontal two dimensions x and y, defined as the distance between the peptide's center of mass and the phospholipid's center of mass, is less than 18 Å). The second group includes 11 phospholipids that are at an intermediate distance from the peptide (horizontal distances between 18 Å and 23.5 Å). The third group includes the last 12 phospholipids, which are the farthest from the peptide (horizontal distances over 23.5 Å). Separate order parameter profiles were calculated for each group. It should be noted that in addition to the advantages for the analysis, this partitioning has the disadvantage of increasing the errors (due to the decrease in sample size).

Fig. 6 depicts the order parameter profiles calculated for the phospholipids in the upper layer of the membrane. Shown are the deuterium order parameters for the phospholipids closest to the peptide in comparison to the order parameters of phospholipids farther away (averaged over the second and third groups) and to the order parameter of the pure DPPC membrane. The order parameters are averaged over the last 300 ps of the simulation. A dramatic effect is seen in the order parameter of the lipids closest to the peptide, which show a significant reduction in S_{CD} values, compared to phospholipids far from the peptide, which exhibit an order parameter profile similar to that of a

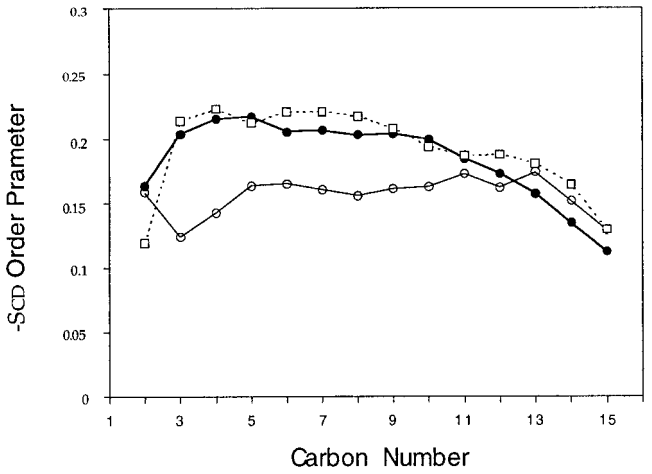

FIGURE 6 The deuterium order parameter profiles $-S_{CD}$ of phospholipids in the upper extracellular layer of the membrane, into which the peptide is inserted. Lipids close to the peptide (first tier) (*solid line with open circles*) and lipids further away from the peptide (second and third tiers) (*dashed line with open squares*). The order parameters are averaged over the last 300 ps of the dynamics simulation. Also shown is the order parameter calculated for the pure DPPC membrane, before the peptide was inserted, average over 100 ps of dynamics (*heavy solid line with filled circles*).

pure bilayer. The average order parameter in the plateau region, between C4 and C8, for the lipids closest to the peptide is $\langle S_{CD}\rangle_{[4,8]} = 0.157 \pm 0.009$ (i.e., standard deviation of 0.009) compared to $\langle S_{CD}\rangle_{[4,8]} = 0.215 \pm 0.006$ for lipids in the second and third tiers, and $\langle S_{CD}\rangle_{[4,8]} = 0.209 \pm 0.006$ for the pure bilayer. A qualitatively similar reduction in order parameter near embedded peptides was observed in the simulation of alamethicin, influenza M2, and OmpF embedded in a POPE membrane (Tieleman et al., 1998). However, in that study the maximum reduction in order parameter, which was in the presence of OmpF, was ~15%, while in the present study the reduction in order parameter near the peptide is greater, almost 25%.

The reduced values of S_{CD} for acyl chains in the immediate vicinity of the peptide may be accounted for in several ways. One explanation is that the decrease in order parameter really reflects an increase in chain disorder near the embedded protein. In this case one expects to find an increase in the rate of dihedral transitions and possibly a larger percentage of *trans/gauche* defects. A second explanation is that the reduced S_{CD} values reflect restricted acyl chain motion, particularly dihedral transitions, near the peptide due to steric hindrance. This results in poor averaging, which may appear as a reduced value of S_{CD} and should be accompanied by a decrease in the rate of dihedral transitions and an unchanged number of *trans/gauche* defects. A third explanation, recently proposed by Tieleman et al. (1998), suggests that the decrease in order parameters close to an embedded peptide is due to a change in the overall tilt of the lipids. They argue that the observed 25–30° tilt can account for the observed 15% decrease in order parameter in the case of OmpF in DOPE. Because the lipid tilt in this study is similar to the above value (see below), it is possible that also in the melittin/DPPC system the tilts contribute ~15% to the reduction in order parameter. A question still remains regarding the origin of the additional 10% reduction in order parameter. As will be discussed below, both the rate of dihedral transitions and the percentage of *gauche* defects in the phospholipids closest to the peptide were similar to those for more distant phospholipids, preventing a clear distinction between the different scenarios. Order parameter values alone are not sufficient to determine whether the upper layer of the bilayer exhibits a higher level of disorder near the peptide. It is likely that significantly longer simulations will be required to settle this question.

An interesting phenomenon is also observed in Fig. 6 at the tail end of the acyl chains. As expected, carbons in the tail region are more disordered than carbons at the plateau region closer to the headgroups. However, in the presence of the peptide we find that for all phospholipids, both close to and far from the peptide, the values of S_{CD} for the C13 to C15 are 15–20% higher than the equivalent values in the pure DPPC bilayer. It seems that the presence of the peptide in the relatively unstructured low-density region, toward the membrane's midsection, slightly increases the order in that region (which is still disordered compared to the plateau region). It is interesting to note that in this region, carbons 13–15, the effect is seen throughout the three tiers of phospholipids.

The dip in the order parameter profile immediately behind the headgroup, $S_{CD} = 0.15–0.17$, seen in both pure and peptide-embedded bilayers, is also observed in NMR experimental data at 350 K, $S_{CD} = 0.16$ (Marrink, 1994; Tieleman et al., 1997). It is likely that the observed low-order parameter at the surface is a consequence of a reduced amount of motion near the interface.

Although the peptide was inserted into the upper extracellular later of the membrane, it also partially penetrates into the lower intracellular layer. In fact, the density profiles depicted in Fig. 2 show that the peptide penetrates as much as 9 Å into the lower layer and as such is likely to affect the order in that part of the system as well. Fig. 7 shows the deuterium order parameter profiles of the phospholipids in the lower layer of the membrane, grouped according to their distance from the peptide. Also shown is the order parameter profile of the pure membrane. With the exception of the order parameter of lipids in the third tier, farthest from the peptide, the deuterium order parameters in the lower layer are qualitatively similar to those in the upper layer. That is, phospholipids closest to the peptide show a dramatic drop in their order parameter values, while lipids in the second tier exhibit an order parameter profile similar to that of a pure bilayer. The corresponding plateau averages are $\langle S_{CD}\rangle_{[4,8]} =$

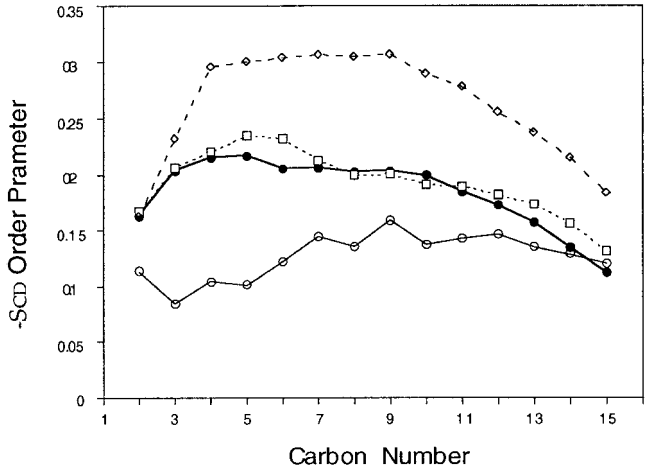

FIGURE 7 The deuterium order parameter profiles $-S_{CD}$ of the phospholipids in the lower intracellular layer of the membrane, similar to Fig. 6. The phospholipids are grouped into three equal size groups according to their distance from the embedded peptide (see text): lipids close to the peptide (first tier) (*solid line with open circles*), lipids further away from the peptide (second tier) (*dashed line with open squares*), and lipids farthest from the peptide (third tier) (*dashed line with open diamonds*). The order parameter for pure membrane is shown for comparison (*heavy solid line with filled circles*).

0.121 ± 0.019 for lipids in the first tier and $\langle S_{CD}\rangle_{[4,8]} = 0.205 \pm 0.016$ for lipids in the second tier.

Three further observations can be made regarding the order parameters of lipids on the intracellular side of the membrane. First, it is interesting to note that those lower-layer lipids, which are close to the peptide, exhibit a sharper decrease in order parameter compared to their counterparts on the extracellular side ($\langle S_{CD}\rangle_{[4,8]} = 0.121 \pm 0.019$ in the lower layer compared to $\langle S_{CD}\rangle_{[4,8]} = 0.157 \pm 0.009$ in the upper layer). This effect is present despite the fact that the peptide penetrates only to the tail region of these lipids. It is not in direct contact with any of the methylene groups that comprise the "plateau" region. In fact, the reduction in order parameter increases significantly for methylene groups that are farthest from the peptide. The average value for carbons C2–C6 in lipids at the first tier in the lower layer is $\langle S_{CD}\rangle_{[2,6]} = 0.105 \pm 0.014$, almost 45% smaller than the equivalent value in the upper layer $\langle S_{CD}\rangle_{[2,6]} = 0.151 \pm 0.017$. However, the average value for carbons C7-C12 is $\langle S_{CD}\rangle_{[7,12]} = 0.144 \pm 0.008$, only 13% lower than the corresponding value in the upper layer, $\langle S_{CD}\rangle_{[7,12]} = 0.162 \pm 0.005$. The fact that the methylene groups that exhibit the strongest effect are not in contact with the peptide indicates that the reduction in order parameter in this case is not due to restricted motion in the vicinity of the peptide. These observations support the conclusion that the observed reduction in S_{CD} may be attributed, to a significant degree, to a real increase in disorder in the lower layer. In addition, lipids in the lower layer adopt only a very small tilt angle relative to the membrane normal (see below), further reducing the role of this tilt as a major source for the observed reduced order parameters.

Second, the increase in order toward the tail end of the chains, which was observed in the upper layer, is less prominent in the lower layer. It is seen mainly in the second tier of lipids. Finally, the most striking peculiarity in the order parameter profiles of lower layer is the order parameter associated with lipids in the third tier, furthest from the peptide. While such lipids in the upper layer behave as if they were part of a pure bilayer, the phospholipids furthest from the peptide (the third tier) in the lower layer exhibit a surprising increase in their order parameter, with a plateau average of $\langle S_{CD}\rangle_{[4,8]} = 0.302 \pm 0.04$, indicating that they are more ordered than in a pure bilayer. This, however, should be considered a nonphysical artifact of the simulation. While we took care to remove two phospholipids from the upper layer to make room for the peptide, no such preparation was made in the lower layer (expecting the peptide to primarily penetrate the low-density interior of the membrane). A consequence of this treatment is an increase in the density at the lower half of the membrane, resulting in artificially increased order near the simulation boundaries.

Finally, to allow comparison with experimental data, an overall order parameter profile averaged over the whole membrane was calculated. The calculated average plateau value for the whole membrane in the presence of the peptide was $\langle S_{CD}\rangle_{[4,8]} = 0.203$. This average is ~3% smaller than the average plateau value calculated from the simulation of the pure bilayer, $\langle S_{CD}\rangle_{[4,8]} = 0.209$. These results should be compared to the NMR experimental data of Dufourc et al. (1986), which indicate that in the presence of melittin the quadropolar splitting of a liquid crystalline DPPC bilayer (at 61°C), which is proportional to the deuterium order parameter, is reduced by ~12% (the effect in the gel phase at 41° was much smaller). The turnover effect at the tail end of the acyl chain, seen in the simulations, was not observed in those NMR experiments. Recently an experimental study by De Planque et al. (1998) of the effect of several transmembrane peptides on various diacylphosphatidylcholine bilayers resulted in very small effects of 17–19-residue α-helices on the order parameter of DPPC at 51° (close to the simulation temperature of 47°).

Free volume in the membrane

Another indicator of the effect of the embedded peptide on the structural properties of the membrane is whether the fractional free volume in the membrane changes as a result of its presence. In general, the fractional free volume inside a biological membrane (in the functional Lα phase) is quite high, reflecting the rather fluid state of this macromolecular ensemble. The "empty" free volume was calculated by placing a grid over the system and counting the percentage of grid points that lay outside of any atom's van der Waals sphere. The grid density was approximately one point per

0.5 Å in the x and y directions, and one point per 0.8 Å in the z direction. The fractional free volume calculated for the hydrocarbon region of the pure DPPC bilayer model (excluding the headgroup region), averaged over 100 ps of molecular dynamics, is 54.0 ± 1%. This value agrees with those computed for a DPPC bilayer in a previous study by Marrink et al. (1996). Using a grid density of about one point per 0.5 Å, they found an average free volume of 40% at the ordered part of the membrane near the interface, and close to 60% free volume at the membrane interior (in that study a slightly finer grid was used).

Initially, embedding the peptide in the membrane did not change the fractional free volumes, indicating that the embedding process did not create artificial cavities in the membrane (cavities could have been created by geometric mismatches between the peptide and the empty space created after removing the two phospholipids from the center of the upper layer). In fact, the same percentage of free volume was maintained during the first 270 ps of the dynamic simulations. During this period the average fractional free volume in the membrane's hydrophobic region was 54.6 ± 1%, similar to that obtained in a pure membrane. Fig. 8 compares the fractional free volume in the lipid region of the bilayer for the last 300 ps of the combined melittin/membrane simulation and in a pure DPPC membrane (for 100 ps of dynamics). At time $t \approx 270$ ps there is a sudden increase in the fraction free volume inside the lipid region of the membrane. After this increase, and for the remainder of the simulation, the fractional free volume inside the lipid region of the membrane stabilizes around a new average value of 57.4 ± 1.4%, almost 3% higher than fractional free volume in the pure membrane. Further analysis showed that the fractional free volume increases in both the upper and lower layers of the membrane. However, the increase in free volume in the lower layer was a little larger than in the upper layer (by ~1%).

Lipid tilts relative to membrane normal

Fig. 1, which depicts the system's conformation at the end of the 500 ps of dynamics, shows the striking correlation between the peptide's tilt and the average tilt of the upper lipid layer. In the above discussion it was shown that in the course of the dynamic simulation the peptide acquires a 24° tilt relative to the membrane normal. Given the elongated nature of the lipid hydrocarbon chains, it is not surprising that the peptide tilt is correlated with the overall orientation of the lipid chains in the membrane. Fig. 9 shows the average tilt of the lipids in the upper and lower layers of the membrane as a function of time. The difference between the two layers is clear. Lipids in the lower layer, which is less perturbed by the peptide, are essentially perpendicular to the membrane surface, exhibiting an average tilt angle of 8° ± 2°. However, one cannot rule out the possibility that the limited tilt in the lower layer may be an artifact cased by the slightly higher density in the lower layer. Lipids in the upper layer, on the other hand, acquire a tilt angle similar to that of the peptide, averaging 24° ± 2° over the last 200 ps of the simulation. Overlaying the average tilt of the membrane and the tilt of the peptide (Fig. 9) shows that these two quantities are highly correlated throughout the simulation. In fact, the correlation between the two curves is such that the average difference between the two curves is only 3.8° ± 2.8°. The tilts observed for the upper layer are similar to the 25–30° tilts reported for other membranes with embedded peptides (Belohorcova et al., 1997; Shen et al., 1997; Tieleman et al., 1998).

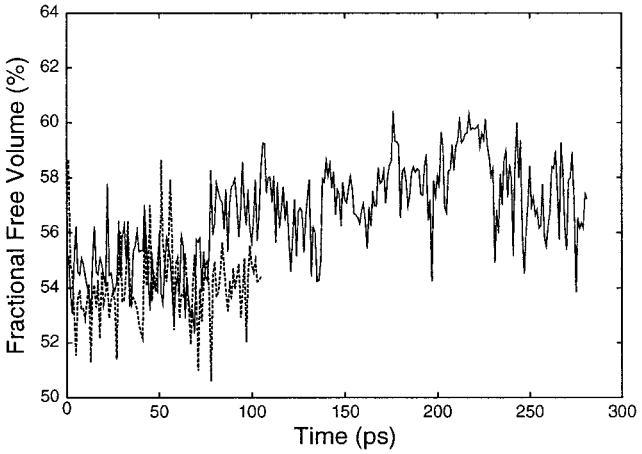

FIGURE 8 The fractional free volume in the lipid region of the membrane bilayer during the last 300 ps of the melittin/membrane simulation (*solid line*) in comparison to 100 ps of a pure DPPC membrane (*dashed line*).

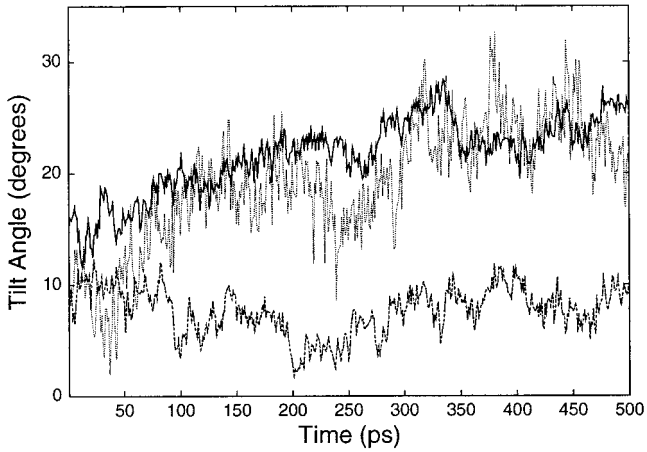

FIGURE 9 The average tilt of the lipid chains in the upper layer (*solid line*) and in the lower layer (*dashed line*) as a function of time. Also shown is the tilt of the peptide (*dotted line*, similar to Fig. 5). Tilt angles are calculated relative to the membrane normal.

Lipid dihedral angles

As discussed above, the dramatic effect of the embedded peptide on the order parameter of the phospholipids closest to it is expected to be reflected in the dynamic properties of the acyl-chain dihedral angles. In biological membranes the lipid chains tend to adopt an extended *trans* conformation, although bends and turns involving local *gauche* conformations are known to occur (see, for example, the very broad CH_3 peak in the systems density plot in Fig. 2). To check for the peptide's influence on the dynamics of lipid chain conformations, we compared the *trans/gauche* tendencies as well as dihedral transition rates for lipids close to the peptide and for lipids far from it. The results did not reveal a clear difference between the two groups, especially as there is a very large variance within each of them. For example, the percentage of *gauche* conformation observed for individual dihedral angles (at the central segment of the lipid chain, during the last 250 ps of the simulation) varied in both groups from 0% to ~55% of the time. Likewise, the rate of dihedral transitions was also characterized by a broad variance. Observed transition rates for individual dihedral angles (at the central segment of the lipid chain) varied from 0 to as much as 15 back-and-forth transitions during the 500 ps of the simulation. No clear difference between lipids close to and far from the peptide was observed. In some cases a high percentage of *gauche* was associated with many back-and-forth transitions between the two conformations (e.g., the dihedral angle defined by carbons C4-C5-C6-C7 of one of the close lipids shown in Fig. 10 *A*, which, all together, exhibits 41% *gauche*). In others, a similar value of *gauche* was associated with a single *trans-gauche* transition, following which the lipid maintained its new conformation (e.g., the dihedral angle defined by carbons C6-C7-C8-C9 of one of the close lipids shown in Fig. 10 *B*, which, all together, exhibits 56% *gauche*).

Surface corrugation

Common to all computer simulations of lipid bilayers is the significant corrugation of the membrane surface. The present study, in which the surface corrugation is between 12 Å (estimated from the width of the phosphorous density profile; Fig. 2) to 14 Å (estimated from the density peak of the glycerol carbons), is no exception to the rule. An interesting question is whether the presence of the embedded peptide effects increases or reduces the corrugation of the membrane surface. For the upper layer, in which the peptide was embedded, the results of the present simulations did not show any significant change in surface corrugation resulting from the presence of the peptide. Changes in the vertical position of the different phospholipids during the dynamic simulation were similar to those observed in the pure bilayer resulting from normal fluctuations. They could not be correlated with the presence of the peptide. The standard deviation in the average vertical position of the headgroups in the upper layer was similar in pure and peptide-hosting membrane models, with the latter exhibiting a slightly smaller degree of fluctuation.

This picture changes for the lower layer of the membrane. A significant degree of deformation was observed in the lower lipid layer near the peptide's N-terminus. Most striking is the response of the phospholipid closest to the N-terminus, which moved deeper into the bilayer. Fig. 11 shows the position of the phosphate atom of this phospholipid as a function of time. It is seen that within the first 200 ps the headgroup of this phospholipid moved as much as 2

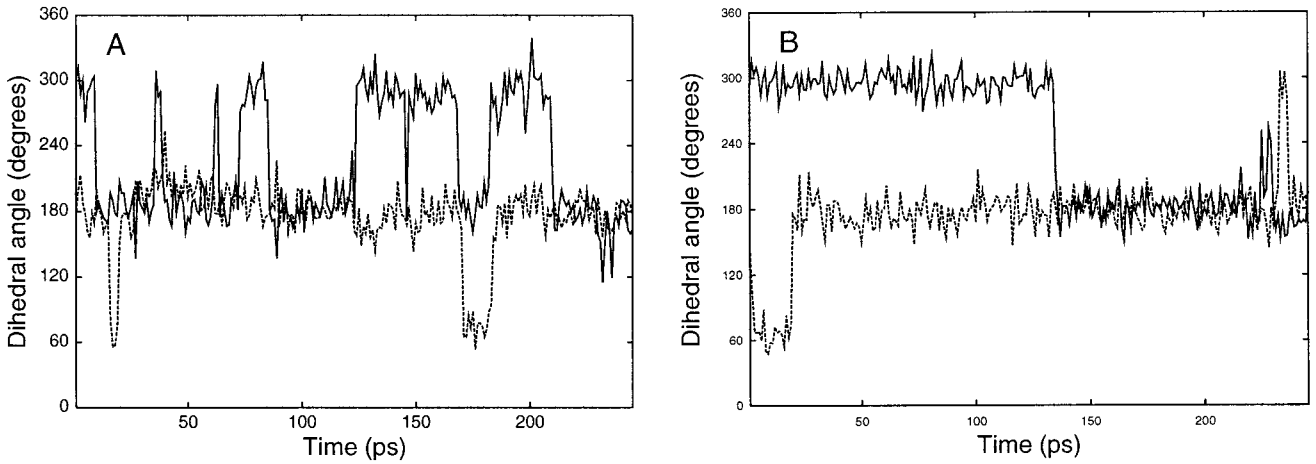

FIGURE 10 Time evolution of specific lipid dihedral angles from phospholipids close to the peptide during the last 250 ps of the simulation. (*A*) Two dihedral angles defined by carbons C4-C5-C6-C7 from the two lipid chains of one of the close lipids (altogether 41% *gauche*). (*B*) Two dihedral angles defined by carbons C6-C7-C8-C9 from the two lipid chains of one of the close lipids (altogether 56% *gauche*), where *gauche* conformations are defined below 120° and above 240°.

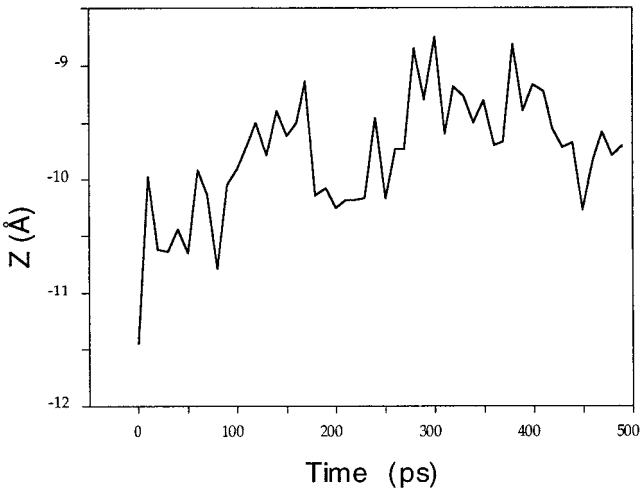

FIGURE 11 The normal z coordinate of the phosphate atom in the phospholipid (from the lower layer) that is closest to the peptide's N-terminus on the intracellular side of the membrane. The headgroup of this phospholipid moves as much as 2 Å into the bilayer.

Å upward into the bilayer (for comparison, its fluctuations in the new location are only ± 0.4 Å). Smaller deformations were observed in a few other phospholipids in that vicinity. This deformation correlates well with observed penetration of water from the intracellular side of the membrane toward the protonated N-terminus of the peptide. A detailed analysis of water penetration into the bilayer in the presence of melittin is presented elsewhere (Bachar and Becker, 1999). In general, water was observed to penetrate from both sides of the membrane within 200 ps of the simulation. From the extracellular side water penetrate toward the charged residue Lys^7, and from the intracellular side water molecules penetrate toward the protonated N-terminus.

The observed surface deformation near the peptide's N-terminus makes it hard to determine the actual width of the membrane in the vicinity of the peptide. No significant change in the overall width of the membrane was observed during the simulation. Experimental studies of the effect of 16–19 residue transmembranal helices on the width of the membrane also resulted in marginal influence on the width of the embedding DPPC bilayer at 51^o (De Planque et al., 1998).

DISCUSSION

The molecular dynamics calculation presented here studies peptide-membrane interaction for the 26-amino acid peptide melittin (with a protonated N-terminus) embedded in a transbilayer orientation in a fully hydrated bilayer consisting of 72 DPPC phospholipids. The simulated membrane is large enough to study the effect of the embedded peptide on the structural properties of the host membrane. Indeed, the peptide's effect was demonstrated in many of the bilayer properties, including deuterium order parameters, fractional free volume, lipid tilts, and surface corrugation.

As reviewed above, one of the putative mechanisms for melittin-induced lysis suggests that this phenomenon occurs through some sort of deformation of the lipid bilayer. A goal of the present simulation was to check this hypothesis and see whether the peptide induces membrane disorder and deformation. A first conclusion from the simulation is that the effect of the peptide on the membrane is local, limited to those phospholipids in its immediate vicinity. This conclusion is in line with the experimental observations of De Planque et al. (1998) and the simulation results of Tieleman et al. (1998).

Interestingly, in this respect we find a difference between the two membrane layers. There is evidence supporting an increased level of disorder in the lower (intracellular) layer of the membrane in the vicinity of the perpendicularly oriented peptide. The increased disorder is indicated by 1) a significant reduction in order parameter close to the peptide's N-terminus, especially for methylene groups that are not in direct contact with the peptide, i.e., toward the intracellular interface; 2) a significant deformation of the intracellular interface just "below" the protonated N-terminus of the peptide; and 3) a preferential increase in the fractional free volume in the lower layer of the membrane (although the upper layer also exhibits an increase in fractional free volume). On the other hand, it seems that the upper, extracellular layer (into which melittin was inserted) is less effected by the embedded peptide. For this layer, however, the results are much less conclusive. The decrease in order parameter of lipids close to the peptide in the upper layer may result from restricted motion due to the peptide's presence or from the lipid's tilt rather than from an increased level of disorder. Furthermore, the decrease in order parameter was not accompanied by an increased rate in dihedral transitions nor by any significant surface deformation of the upper interface.

Alternatively phrased, it seems that the origin of the asymmetrical effect of melittin on the surrounding membrane may be the fact that melittin is *not* a transmembranal helix. Rather, it is anchored only at the extracellular surface of the membrane, spanning no more than two-thirds of the bilayer's width. As a result, melittin's protonated N-terminus is loose in the lower layer of the membrane, leading to an increased amount of disorder in lower-layer phospholipids near the peptide. On the other hand, being anchored at the extracellular interface, melittin has a smaller effect on the structural properties of this layer. Recall that the effect of melittin on the surrounding membrane, in both layers, was localized to its immediate vicinity. In general, the simulation supports a role for local deformation of the phospholipid bilayer in the mechanism of melittin-induced lysis, possibly in relation to water penetration (Bachar and Becker, 1999).

In this respect, melittin is different from the other membrane-embedded peptides studied so far by MD simulations. In most other studies, the embedded peptides were transmembranally anchored in both intra- and extracellular sides of the membrane (Belohorcova et al., 1997; Shen et al., 1997; Tieleman et al., 1998, 1999; Woolf, 1997, 1998; Woolf and Roux, 1996). This double anchor is probably why in these systems the reduction in order parameter near the peptide is smaller compared to that observed in the case of melittin (Shen et al., 1997; Tieleman et al., 1998, 1999). These conclusions should, of course, be restricted to the time scale of the simulation.

An important issue is the role of melittin's membrane binding orientation on lysis and on membrane deformation. As discussed above, the orientational transition from the initial parallel orientation, in which melittin is bound on the surface, to a transbilayer orientation is beyond the scope of today's MD simulations. However, insight into this issue can be obtained by comparing the results of the present study, in which melittin is embedded in a transbilayer orientation, to the recent simulation of Berneche et al. (1998), in which melittin was oriented parallel to the surface. At first glance, the two simulation results appear to be quite different. In the parallel binding orientation the order of the lipid chains in the upper layer was reduced relative to their order in the lower layer (Berneche et al., 1998). In the transbilayer orientation the reverse occurs—the order in the lower layer is reduced relative to the order in the upper layer. In fact, the two observations are a manifestation of the same phenomenon. Phospholipid acyl chains that are close to a loosely bound peptide are affected by it and become less ordered (i.e., in the upper layer when the peptide is in a parallel orientation, or in the lower layer when the peptide is in a transbilayer orientation). Otherwise the effect is negligible (i.e., the lower layer is not in contact with the peptide when it is in a parallel orientation, and the upper layer is less affected when melittin is anchored in the transbilayer orientation). In any case, both simulations attest to the remarkable plasticity of the membrane, which adapts to the presence of melittin.

As for other properties, the melittin in the bilayer behaves much like any other membrane-embedded polypeptide. Most notably, melittin adopts a significant tilt of up to 25° relative to the membrane normal. Such tilts were also reported for other membrane-embedded peptides (Belohorcova et al., 1997; Shen et al., 1997; Tieleman et al., 1998). In melittin, the peptide's tilt is strongly correlated with a similar tilt of the lipids in the upper layer of the membrane. Lipids in the lower layer, however, do not exhibit a similar tilt. This, again, may be a consequence of the fact that melittin is not a transmembranal helix. The decoupling of the lower layer from the upper layer is assisted by the presence of the peptide's intrahelix bend right at the bilayer's midsection. It should be noted, however, that the limited tilt in the lower layer may be an artifact of the simulation caused by the slightly higher density in the lower layer.

The peptide itself retains its overall helical structure throughout the simulation. With the exception of the three N-terminal amino acids (Gly^1-Ile^2-Gly^3), structural integrity of the peptide is maintained during the dynamics. In particular, there is no "unwinding" of the helix at the peptide's C-terminus. The characteristic intrahelical bend of melittin adopts a value close to 30° immediately at he beginning of the simulation and is then maintained throughout.

Finally, the present simulation, like other MD studies of membrane systems, is limited by the system size and the simulation time scale. A full characterization of the melittin/bilayer system would require extensive ensemble averaging as well as simulations much longer than is possible on today's computers (with extreme effort MD simulations of a system of this size can reach the order of 10 ns). This means that MD simulations cannot directly address the intriguing question regarding the stability, whether transient or stable, of the perpendicular orientation of melittin (with a charged N-terminus). The physical process associate with this transition takes place on a much longer time scale. For the same reason, these simulations cannot directly address the possible formation of melittin aggregates. Nonetheless, the present results shed more light on the detailed interplay between the embedded peptide and the bilayer, and support at least in part the possible roles of membrane deformation and water penetration in melittin lysis. Together with the complementary study of melittin in the parallel orientation (Berneche et al., 1998), a fuller picture of this system is starting to emerge.

We are grateful to R.W. Pastor and S. E. Feller for allowing us to use their equilibrated model of a pure DPPC bilayer, as well as for much helpful advice.

This study was supported in part by a grant from the Israel Science Foundation and by a grant from the Israeli Inter-University Supercomputing Center.

REFERENCES

Alper, H. E., and T. R. Stouch. 1995. Orientation and diffusion of a drug analogue in biomembranes: molecular dynamics simulations. *J. Phys. Chem.* 99:5724–5731.

Bachar, M., and O. M. Becker. 1999. Melittin at a membrane/water interface: effects on water orientation and water penetration. *J. Chem. Phys.* 111:8672–8685.

Bazzo, R., M. J. Tappin, A. Pastore, T. S. Harvey, J. A. Craver, and I. D. Campbell. 1988. The structure of melittin: a ^{1}H-NMR study in methanol. *Eur. J. Biochem*. 173:139–146.

Belohorcova, K., J. H. Davis, T. B. Woolf, and B. Roux. 1997. Structure and dynamics of an amphiphilic peptide in a lipid bilayer: a molecular dynamics study. *Biophys. J.* 73:3039–3055.

Berger, O., O. Edholm, and F. Jahnig. 1997. Molecular dynamics simulations of a fluid bilayer of dipalmitoylphosphatidylcholine at full hydration, constant pressure, and constant temperature. *Biophys. J.* 72: 2002–2013.

Berneche, S., M. Nina, and B. Roux. 1998. Molecular dynamics simulation of melittin in a dimyristoylphosphatidylcholine bilayer membrane. *Biophys. J.* 75:1603–1618.

Bradrick, T. D., A. Philippetis, and S. Georghiou. 1995. Stopped-flow fluorometric study of the interaction of melittin with phospholipid bilayers: importance of the physical state of the bilayer and the acyl chain length. *Biophys. J.* 69:1999–2010.

Bradshaw, J. P., C. E. Dempsey, and A. Watts. 1994. A combined x-ray and neutron diffraction study of selectively deuterated melittin in phospholipid bilayers: effect of pH. *Mol. Membr. Biol.* 11:79 -86.

Brooks, B. R., R. E. Bruccoleri, B. D. Olafson, D. J. States, S. Swaminathan, and M. Karplys. 1983. CHARMM: a program for macromolecular energy, minimization, and dynamics calculations. *J. Comput. Chem.* 4:187–217.

Chiu, S.-W., M. Clark, S. Subramanian, H. L. Scott, and E. Jakobsson. 1995. Incorporation of surface tension into molecular dynamics simulations at interfaces: a fluid phase lipid bilayer membrane. *Biophys. J.* 69:1230–1245.

Damodaran, K. V., and K. M. Merz, Jr. 1994. Computer simulation of lipid systems. *In* Reviews in Computational Chemistry. K. B. Lipkowitz and D. B. Boyd, Editors. VCH Publishers, New York.

Damodaran, K. V., K. M. Merz, Jr., and B. P. Gaber. 1995. Interaction of small peptides with lipid bilayers. *Biophys. J.* 69:1299–1308.

DeGrado, W. F., G. F. Musso, M. Lieber, E. T. Kaiser, and F. J. Kezdy. 1982. Kinetics and mechanism of hemolysis induced by melittin and by a synthetic melittin analogue. *Biophys. J.* 37:329–338.

De Planque, M. R. R., D. V. Greathouse, R. E. Koeppe, II, H. Schäfer, D. Marsh, and J. A. Killian. 1998. Influence of lipid/peptide hydrophobic mismatch on the thickness of diacylphosphatidylcholine bilayers. A ^{2}H NMR and ESR study using designed transmembrane α-helical peptides and gramicidin A. *Biochemistry.* 37:9333–9345.

Dempsey, C. E. 1990. The actions of melittin on membranes. *Biochim. Biophys. Acta.* 1031:143–161.

Devaux, P. F., and M. Siegneuret. 1985. Specificity of lipid-protein interactions as determined by spectroscopic techniques. *Biochim. Biophys. Acta.* 822:63–125.

Douliez, J. P., A. Leonard, and E. J. Dufourc. 1995. Restatement of order parameters in biomembranes: calculation of C-C bond order parameters from C-D quadrupolar splittings. *Biophys. J.* 68:1727–1739.

Ducarme, P., M. Rahman, and B. Brasseur. 1998. IMPALA: a simple restraint field to simulate the biological membrane in molecular structure studies. *Proteins.* 30:357–371.

Dufourc, E. J., I. C. P. Smith, and J. Dufourcq. 1986. Molecular details of melittin-induced lysis of phospholipid membranes as revealed by deuterium and phosphorus NMR. *Biochemistry.* 25:6448–6455.

Feller, S. E., and R. W. Pastor. 1996. On simulating lipid bilayers with an applied surface tension: periodic boundary conditions and undulations. *Biophys. J.* 71:1350–1355.

Feller, S. E., R. W. Pastor, A. Rojnickarin, S. Bogusz, and B. R. Brooks. 1996. Effect of electrostatic force truncation on interfacial and transport properties of water. *J. Phys. Chem.* 100:17011–17020.

Feller, S. E., R. M. Venable, and R. W. Pastor. 1997. Computer simulations of a DPPC phospholipid bilayer: structural changes as a function of molecular surface area. *Langmuir.* 13:6555–6561.

Feller, S. E., Y. Zhang, R. W. Pastor, and B. R. Brooks. 1995. Constant pressure molecular dynamics simulation: the Langevin piston method. *J. Chem. Phys.* 103:4613–4621.

Geve, G., and D. March. 1987. Phospholipid Bilayers: Physical Principles and Models. Wiley Interscience, New York.

Gevod, V. S., and K. S. Birdi. 1984. Melittin and the 8–26 fragment: differences in ionophoric properties as measured by monolayer method. *Biophys. J.* 45:1079–1083.

Habermann, E., and H. Kowallek. 1970. Modification of amino groups and tryptophan in melittin as an aid to recognition of structure-activity relationships. *Hoppe Seylers Z. Physiol. Chem.* 351:884–890.

Heller, H., M. Schaefer, and K. Schulten. 1993. Molecular dynamics simulation of a bilayer of 200 lipids in the gel and in the liquid-crystal phases. *J. Phys. Chem.* 97:8343–8360.

Jost, P., O. H. Griffith, R. A. Capaldi, and G. Vanderkooi. 1973. Evidence for boundary lipid in membrane. *Proc. Natl. Acad. Sci. USA.* 70: 480–484.

Koynova, R., and M. Caffrey. 1998. Phases and phase transitions of the phosphatidylcholines. *Biochim. Biophys. Acta.* 1376:91–145.

Lopez Cascales, J. J., J. Garcia de la Torre, S. J. Marrink, and H. J. C. Berendsen. 1996. Molecular dynamics simulation of a charged biological membrane. *J. Chem. Phys.* 104:2713–2720.

MacKerell Jr., A. D., D. Bashford, M. Bellott, R. L. Dunbrack, Jr., J. D. Evanseck, M. J. Field, S. Fischer, J. Gao, H. Guo, S. Ha, D. Joseph-McCarthy, L. Kuchnir, K. Kuczera, F. T. K. Lau, C. Mattos, S. Michnick, T. Ngo, D. T. Nguyen, B. Prodhom, W. E. Reiher III, B. Roux, M. Schlenkrich, J. C. Smith, R. Stote, J. Straub, M. Watanabe, J. Wiorkiewicz-Kuczera, D. Yin, and M. Karplus. 1998. All-atom empirical potential for molecular modeling and dynamics studies of proteins. *J. Phys. Chem. B.* 102:3586–3616.

Manjunatha-Kini, R., and H. J. Evans. 1989. A common cytolytic region in myotoxins, hemolysins, cardiotoxins and antibacterial peptides. *Int. J. Pept. Protein Res.* 34:277–286.

Marrink, S. J. 1994. Permeation of Small Molecules across Lipid Membranes. Ph.D. thesis, University of Groningen.

Marrink, S. J., and H. J. C. Berendsen. 1994. Simulation of water transport through a lipid membrane. *J. Phys. Chem.* 98:4155- 4168.

Marrink, S. J., O. Berger, P. Tieleman, and F. Jahnig. 1998. Adhesion forces of lipids in a phospholipid membrane studied by molecular dynamics simulations. *Biophys. J.* 74:931–943.

Marrink, S. J., R. M. Sok, and H. J. C. Berendsen. 1996. Free volume properties of a simulated lipid membrane. *J. Chem. Phys*. 104: 9090–9099.

Milik, M., and J. Skolnick. 1993. Insertion of peptide chains into lipid membranes: an off-lattice Monte Carlo dynamics model. *Proteins Struct. Funct. Genet.* 15:10–25.

Monette, M., and M. Lafleur. 1995. Modulation of melittin-induced lysis by surface charge density of membranes. *Biophys. J.* 68:187–195.

Mouritsen, O. G. 1991. Theoretical models of phospholipid phase transition. *Chem. Phys. Lipids.* 57:178–194.

Mouritsen, O. G., and R. L. Biltonen. 1993. Protein-lipid interactions and membrane heterogeneity. *In* Protein-Lipid Interactions. A. Watts, editor. Elsevier, London. 1–39.

Nagle, J. F., R. Zhang, S. Tristram-Nagle, W. Sun, H. I. Petrache, and R. M. Suter. 1996. X-ray structure determination of fully hydrated L alpha phase dipalmitoylphosphatidylcholine bilayers. *Biophys. J.* 70: 1419–1431.

Pastor, R. W. 1994. Molecular dynamics and Monte Carlo simulations of lipid bilayers. *Curr. Opin. Struct. Biol.* 4:486–492.

Pastore, A., T. S. Harvey, C. E. Dempsey, and I. D. Campbell. 1989. The dynamic properties of melittin in solution: investigation by NMR and molecular dynamics. *Eur. Biophys. J.* 16:363–367.

Ruggiero, A., and B. Hudson. 1989. Critical density fluctuations in lipid bilayers detected by fluorescence lifetime heterogeneity. *Biophys. J.* 55:1111–1124.

Schlenkrich, M., J. Brickman, A. D. MacKerell, and M. Karplus. 1996. An empirical potential energy function for phospholipids: criteria for parameter optimization and applications. *In* Biological Membranes: A Molecular Perspective from Computation and Experiment. K. Merz and B. Roux, editors. Birkhäuser, Boston, MA.

Scott, H. L. 1986. Monte Carlo calculations of order parameter profiles in models of lipid-protein interactions in bilayers. *Biochemistry.* 25: 6122–6126.

Scott, H. L., and S. Kalaskar. 1989. Lipid chains and cholesterol in model membranes: a Monte Carlo study. *Biochemistry.* 28:3687–3691.

Seelig, A., and J. Seelig. 1974. The dynamic structure of fatty acyl chains in a phospholipid bilayer measured by deuterium magnetic resonance. *Biochemistry.* 13:4839–4845.

Shen, L. Y., D. Bassolino, and T. Stouch. 1997. Transmembrane helix structure, dynamics, and interactions: multi-nanosecond molecular dynamics simulations. *Biophys. J.* 73:3–20.

Terwilliger, T. C., and D. Eisenberg. 1982. The structure of melittin. II. Interpretation of the structure. *J. Biol. Chem.* 257:6016–6022.

Tieleman, D. P., and H. J. C. Berendsen. 1996. Molecular dynamics simulations of a fully hydrated dipalmitoyl phosphatidylcholine bilayer with different macroscopic boundary conditions and parameters. *J. Chem. Phys.* 105:4871–4880.

Tieleman, D. P., and H. J. C. Berendsen. 1998. A molecular dynamics study of the pores formed by *Escherichia coli* OmpF porin in a fully hydrated palmitoyloleoylphosphatidylcholine bilayer. *Biophys. J.* 74: 2786–2801.

Tieleman, D. P., L. R. Forrest, M. S. P. Sansom, and H. J. C. Berendsen. 1998. Lipid properties and the orientation of aromatic residues in OmpF, influenza M2 and alamethicin systems: molecular dynamic simulations. *Biochemistry.* 37:17554–17561.

Tieleman, D. P., S. J. Marrink, and H. J. C. Berendsen. 1997. A computer perspective of membranes: molecular dynamics studies of lipid bilayer systems. *Biochim. Biophys. Acta.* 1331:235–270.

Tieleman, D. P., M. S. P. Sansom, and H. J. C. Berendsen. 1999. Alamethicin helices in a bilayer and in solution: molecular dynamics simulations. *Biophys. J.* 76:40–49.

Tosteson, M. T., S. J. Holmes, M. Razin, and D. C. Tosteson. 1985. Permeation of ions in membranes. *J. Membr. Biol.* 87:35–44.

van der Ploeg, P., and H. J. C. Berendsen. 1982. Molecular dynamics of a bilayer membrane. *J. Chem. Phys.* 76:3271–3276.

Vogel, H. 1987. Comparison of the conformation and orientation of alamethicin and melittin in lipid membranes. *Biochemistry.* 26:4562–4572.

Vogel, H., and F. Jähnig. 1986. The structure of melittin in membranes. *Biophys. J.* 50:573–582.

Weaver, A. J., M. D. Kemple, J. W. Brauner, R. Mendelsohn, and F. G. Prendergast. 1992. Fluorescence, CD, attenuated total reflectance (ATR) FTIR and ^{13}C NMR characterization of the structure and dynamics of synthetic melittin and melittin analogues in lipid environments. *Biochemistry.* 31:1301–1313.

Woolf, T. B. 1997. Molecular dynamics of individual alpha-helices of bacteriorhodopsin in dimyristoyl phosphatidylcholine. 1. Structure and dynamics. *Biophys. J.* 73:2376–2392.

Woolf, T. B. 1998. Molecular dynamics of individual alpha-helices of bacteriorhodopsin in dimyristoyl phosphatidylcholine. 2. Interaction energy analysis. *Biophys. J.* 74:115–131.

Woolf, T. B., and B. Roux. 1996. Structure, energetics, and dynamics of lipid-protein interactions: a molecular dynamics study of the gramicidin A channel in a DMPC bilayer. *Proteins.* 24:92–114.